Improving Radio Transmission Through a Dense Plasma via Electron-Neutral Collisions

Vijay Harid, Daniel Main, Mark Gołkowski, Aakash Sahai, Joshua Wewerka, Sri T.R. Chilukury, and Egduard Jauregui

Abstract – Radio transmission through ionized media is a common requirement in several applications, including high-speed vehicles traveling in Earth's atmosphere and ionosphere. The plasma surrounding a vehicle prevents efficient radiation at typical radio frequencies. Investigating potential methods to improve transmission efficiency is thus an active area of research. Here, the role of electron-neutral collisions is investigated. It is first shown that for a simplified model of a homogeneous plasma slab, electron-neutral collisions can considerably improve radio transmission below the plasma frequency. Improved transmission at low frequencies due to collisions is confirmed in a realistic inhomogeneous case using an finite difference time domain simulation, thus demonstrating a potential strategy for circumventing shielding from plasma. Although electron-neutral collisions are typically associated with elevated radio wave absorption in plasmas, for frequencies below the plasma frequency, collisions enhance transmission through ionized media, yielding a "collision frequency window."

1. Introduction

High-speed aerial vehicles often experience plasma formation around the structure. In such conditions, radio wave transmission can be considerably impaired due to the electromagnetic properties of the plasma. In particular, electromagnetic waves below the plasma frequency are shielded, resulting in diminished power transmission. Although this problem has been well studied for multiple decades, a comprehensive solution has been elusive, and several approaches for mitigating the radio attenuation problem are still being investigated [1–6]. One approach is the injection of an electrophilic gas that serves to absorb free electrons and reduce the electron density [5]. Another approach is the so-called magnetic window [4], where magnetizing the plasma with onboard magnets permits access to plasma wave modes that can propagate below the plasma frequency. Although a theoretically viable strategy, the large magnetic fields required at typical radio frequencies can be difficult to practically achieve.

Manuscript received 10 November 2022.

Vijay Harid, Mark Gołkowski, Aakash Sahai, Joshua Wewerka, Sri T. R. Chilukury, and Egduard Jauregui are with the Department of Electrical Engineering, University of Colorado Denver, 1200 Larimer Street, Denver, Colorado 80204; e-mail: mark.golkowski@ucdenver.edu.

Daniel Main is with TechX Corporation, 5621 Arapahoe Avenue, Suite A, Boulder, Colorado 80303; e-mail: dmain@txcorp.com.

Another electromagnetic-based strategy is to surround the vehicle in a double-positive medium metamaterial to match the impedance of the plasma and allow for improved radio transmission [6]. Concerns with this method include the direct interaction with plasma particles as well as the complex changes to the radiation pattern of the antennas. Due to these challenges, a multimodal approach to mitigating radio blackout is likely needed, and introducing novel techniques can assist in achieving an eventual holistic solution.

We focus on radio frequencies from 100 MHz to 40 GHz and consider the role of electron-neutral collisions in the transmission of a plane wave through a dense, collisional plasma. In particular, a finite collision frequency introduces losses to the system and alters the transmission characteristics. Utilizing lossy waveguides is a well-established technique for improving impedance matching in microwave circuits; the novelty of the present work is to leverage a similar concept but for transmission through a finite plasma medium. In Section 2, we set up the theoretical treatment. In Section 3, we discuss the simulation setup and present results that demonstrate the validity of the model. In Section 4, we show agreement between theory and simulation, thus validating both methods. Finally, in Section 5, we consider the case of a more realistic plasma density profile based on fluid modeling of a high-speed vehicle.

2. Plasma Transmission Theory

In the absence of a background magnetic field, the effective relative permittivity of plasma media is given by

$$\epsilon_r = 1 - \frac{\left(\frac{\omega_p}{\omega}\right)^2}{1 - \frac{j\nu}{\omega}} \tag{1}$$

where the quantities ω_p, ν, and ω represent the plasma frequency, electron collision frequency, and radio wave frequency, respectively. Electron-neutral collisions are dominant in weakly ionized plasmas dominated by neutrals, which is the case for most plasmas present or excited in the atmosphere and ionosphere. A fully ionized plasma would experience electron-ion collisions dominated by Coulomb forces.

In the absence of collisions ($\nu = 0$), the plasma frequency marks an abrupt transition separating propagating ($\omega > \omega_p$) and purely evanescent waves ($\omega \leq \omega_p$). Physically, the electric and magnetic fields are perfectly out of phase and hence decoupled for frequencies below the plasma frequency. The inclusion

of collisions introduces damping due to ohmic heating while simultaneously recoupling the electric and magnetic fields. Specifically, finite collision frequencies may still allow for signal transmission through plasmas at low frequencies but with a decay rate that is slower than that of purely evanescent waves.

Calculating the amount of electromagnetic power that propagates through an arbitrarily shaped distribution of plasma will in general require a numerical approach. However, in order to gain relevant physical insight, a closed-form expression for the transmission coefficient is presented in a one-dimensional system.

1.1 Transmission Coefficient for Plane Waves

The simplest approach for estimating the fields transmitted through a collisional plasma is with one-dimensional plane wave analysis. Specifically, consider an infinite slab of homogeneous plasma that is illuminated by a plane wave at normal incidence. The characteristic wave impedance within the plasma is given by $\eta_p = \sqrt{\mu_0/\epsilon_r}$, where ϵ_r is the plasma permittivity shown in (1). As such, the transmission coefficient at the "exit" of the plasma slab can be computed via transmission line theory as given in [7]. The closed-form expression for the transmission coefficient is given by

$$T = \left[\cosh(\gamma d) + \frac{1}{2}\left(\frac{\eta_0}{\eta_p} + \frac{\eta_p}{\eta_0}\right)\sinh(\gamma d)\right]^{-1} \qquad (2)$$

The quantities η_0 and d represent the intrinsic impedance of free space ($\eta_0 = \sqrt{\frac{\mu_0}{\epsilon_0}} \approx 377$ ohms) and the thickness of the slab, respectively. The parameter γ is the complex propagation constant and is given by $\gamma = \frac{j\omega\sqrt{\epsilon_r}}{c}$. The expression in (2) includes the losses due to reflection at the incident interface, multiple internal reflections within the slab, and damping due to ohmic dissipation.

Figure 1 shows the magnitude of the transmission coefficient for a 5 cm plasma slab for both the collisional and the collision-free scenario. The plasma frequency is 21.9 GHz (shown in red, corresponding to an electron density of $6 \times 10^{18}\text{cm}^{-3}$), and the collision frequency is 4.2 GHz. These representative values were chosen since they are in the typical range of parameters expected from fluid simulations of high-speed vehicles. As shown, for frequencies above the plasma frequency, transmission rapidly goes to unity, and the plasma effectively becomes transparent. Below the plasma frequency, the collisional and collision-free cases show opposing trends. As frequency is decreased, the collision-free plasma becomes increasingly opaque, while in the collisional case, it becomes more transparent. As described below, in the low-frequency limit, the plasma begins to act like a classical conductor where lower frequencies undergo less attenuation. Thus, the inclusion of collisions considerably improves the transmission through the plasma slab at frequencies considerably below the plasma frequency.

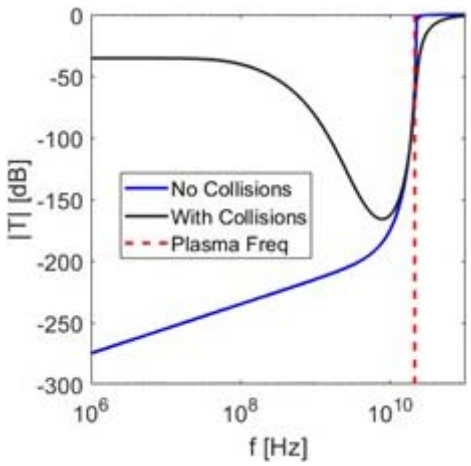

Figure 1. Comparison of transmission coefficient for a plasma slab with and without collisions. The plasma frequency is 21.9 GHz, the collision frequency is 4.2 GHz, and the slab is 5 cm thick.

The expression for the transmission coefficient shown in (2) is for the case of a single homogeneous slab and is thus analytically tractable. Realistic plasmas, however, have an inhomogeneous density profile. The following section describes the simulation methodology for modeling an inhomogeneous plasma.

3. Numerical Simulation Method

We utilize a well-developed finite difference time domain software package called VSim [8]. The plasma is modeled using a frequency-dependent linear plasma dielectric model [9], which is one of the models available in VSim. The simulation domain is established on a two-dimensional Cartesian grid that extends from $y_{\min} - 2\lambda_{EM} < y < y_{\max} + 2\lambda_{EM}$, where λ_{EM} is the wavelength of the EM wave and $2\lambda_{EM}$ is the length of the matched absorbing boundary layer [10]. Absorbing boundary conditions are used to reduce reflections of the EM wave. We set $y_{\min} = -y_{\max} \geq \lambda_{EM}/2$ for all simulations so that the total length exceeds the EM wavelength. The boundary conditions in the x-direction are periodic, extending from $x_{\min} < x < x_{\max}$, where $x_{\min} = -x_{\max} = -0.25$ m. The incident fields are generated by specifying E_x at $y = 0$, launching a plane wave that travels in the y-direction.

The time-dependent source term is given by

$$s(t) = E_0\left(0.5 + 0.5\text{erf}\left(C_0 + \frac{ft}{N}\right)\right)\sin(\omega t) \qquad (3)$$

where f is the linear frequency, $\omega = 2\pi f$, and erf is the error function. The constant C_0 and N are chosen in such a way that the function ramps up over $2 \times |C_0| \times N$ periods. We have set C_0 to -8.0 and N to 4.0, resulting in the ramp-up time of 64 periods. In any finite time domain model as well as in real experiments, the Fourier transform of $s(t)$, which we call $s(\omega)$, peaks at

the excitation frequency (ω_0) and falls off at some rate away from ω_0. We call any wave power not contained in $\omega_0 \pm 2\delta\omega$ the background signal, which we desire to minimize. Since $\delta\omega = 1/(N \times dt)$, the background signal can be reduced by increasing the number of periods that the simulation is run for. The background signal is further reduced by using erf as a ramp-up function. For all the results shown in this report, each simulation has been run for 100 periods.

4. Comparison of Theory and Simulations

We validate the theory and simulations by direct comparison. Since the analytical treatment is limited to a slab geometry, we first present simplified simulation results using parameters typical of flight at 61 km altitude and velocity of 7,650 m/s [11]. The plasma density is set to a constant value of $10^{19}/\text{m}^3$ in the region 0.02 m $< y <$ 0.04 m. The transmission coefficient of a plane wave is computed by comparing the free space field values with the field values after traveling through the plasma dielectric. The extent of the plasma dielectric in the x-direction is the entire length of the simulation domain along x.

The EM dispersion relation in a collisionless plasma is given by $k = \frac{1}{c}\sqrt{\omega^2 - \omega_p^2}$, where ω_p is the plasma frequency and k is the wavenumber. Therefore, in a collisionless plasma, k is purely imaginary for $\omega < \omega_p$, and the EM wave attenuates over a characteristic length called the plasma skin depth given by $\delta = 1/k_i$. The largest value of δ is found be setting $\omega = 0$ and is found to be 1.6 mm. A typical rule for accurate modeling would be for $dx \sim \delta/10$. However, this would result in an extremely high computational cost for the simulations considered in this study. Simulation results have been compared in which we set $dx =$ 0.2 mm, 0.4 mm, 1 mm, and 2 mm. We find reasonable agreement for the three smallest values of dx and therefore designated a grid size of $dx = dy = 1$ mm.

The transmission coefficient is computed in the frequency domain from the ratio of wave power with and without the plasma dielectric in the band $\omega_0 \pm 2\delta\omega$, where ω_0 is the excitation frequency and $\delta\omega$ is the numerical frequency resolution, $\delta\omega = 1/(N \times dt)$. Figure 2 shows the comparison between theory and simulation of a collisionless plasma for 13 different values of ω_0 ranging from 500 MHz to 40 GHz. We decreased the grid size and time step for the 40 GHz simulation in order to adequately resolve this high-frequency RF source. As shown, good agreement is found between simulation and theory. As expected, the transmission improves (approaching a value of 1) as the frequency approaches the plasma frequency at 28 GHz but is severely attenuated below the plasma frequency.

Having investigated transmission of a plane wave through a dense *collisionless* plasma, we now show that electron-neutral collisions significantly improve the transmission of an EM signal through a dense *collisional* plasma. Figure 3 shows the transmission as a function of collision frequency for three RF frequencies: 2 GHz, 6 GHz, and 15 GHz. These three frequencies are chosen to demonstrate the difference in transmission at different RF frequencies, and the chosen values have no special significance. The horizontal axis represents the collision frequency normalized to the ~28 GHz plasma frequency. The discrete collision frequencies, which we specify in VSim, are the following numerical values: $f_{\text{coll}} \approx [0, 4.2, 21, 42, 125]$ GHz, which corresponds to $f_{\text{coll}}/f_{\text{pe}} \approx = [0, 0.15, 0.74, 1.48, 4.43]$. The neutral densities corresponding to these collision frequency values are $\sim [0, 10^{23}, 5 \times 10^{23}, 10^{24}, 3 \times 10^{24}]$ m^{-3}. Both simulation and theory show a perhaps counterintuitive result that increased electron-neutral collisions improve the transmission over all RF frequencies below the plasma frequency. Likewise, the frequency dependence becomes opposite for that in the collisionless case. Namely, transmission is greater at an RF frequency of 2 GHz compared with 6 GHz and 15 GHz above a fairly small value for the collision frequency ($f_{\text{coll}}/f_{\text{pe}} \sim 0.5$). At 2 GHz, transmission at $f_{\text{coll}}/f_{\text{pe}} \cong 4.4$ is ~27,000 times greater compared with $f_{\text{coll}} = 0$.

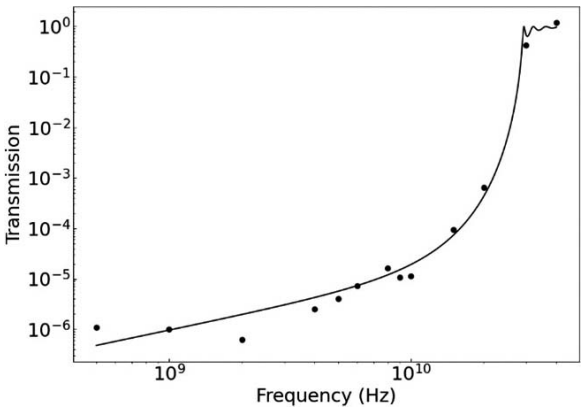

Figure 2. Transmission of an electric monopole antenna through a 2 cm thick collisionless plasma with plasma frequency of 28 GHz. Attenuation is very high below the plasma frequency. Dots represent VSim data, and the solid curve represents theory.

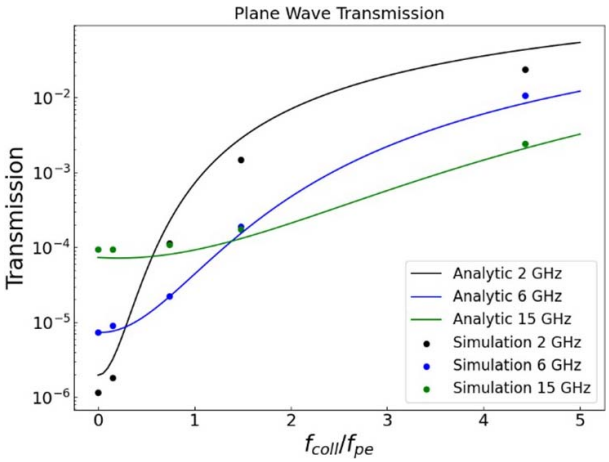

Figure 3. Transmission as a function of collision frequency for three different RF frequencies and a plasma frequency of 28 GHz. Dots represent VSim data, and the solid curves represent theory.

One way to understand the effect of collisions is to treat the plasma as a conducting material. In this case, the skin depth is given by

$$\delta = \left(\frac{2}{\mu\omega\sigma_c}\right)^{1/2} \tag{4}$$

where σ_c is the conductivity, which depends inversely on the electron-neutral collision frequency. Equation (4) shows that as ω decreases, the skin depth and hence transmission increase. Since an increased collision frequency decreases the conductivity, it also increases the skin depth. Thus, skin depth and penetration are maximized for low frequencies and high collision rates.

5. Transmission Through a Realistic Density Profile

The numerical model is now extended to an inhomogeneous density profile due to high-speed flight that is calculated from a computational fluid dynamics simulation package called USim [12]. The vehicle is modeled at an altitude of 61 km, traveling at Mach 23 with a 9-degree pitch angle in the x-y plane. Figure 4 shows a two-dimensional color contour plot of electron density surrounding the RAM C [11] flight modeled in USim in the x-y plane at $z = 0$. The black line represents a one-dimensional cut for which the electron density profile is shown in the bottom panel.

The data from USim shown in Figure 4 are fit to the following function:

$$n_{fit}(x) = n_0 \mathrm{H}(x_{uc} - x)\mathrm{H}(x - x_{lc}) + n_0 \mathrm{H}(x - x_{uc})\exp\left(\frac{-(x - x_{uc})^2}{\delta^2}\right) \tag{5}$$

where H is the Heaviside step function and x_{lc} is the lower cutoff used to move the plasma dielectric away from the antenna placed at $x = 0$ m. The numerical values used in (5) are the following: $x_{lc} = 2$ cm, $x_{uc} = 4.5$ cm, $n_0 = 10^{19}$ cm^{-3}, and $\delta = 5$ cm. Other lineouts could have been cut through the data, but we have chosen the one shown to demonstrate the role of collisions in a realistic density profile.

We next show a plot of transmission versus collision frequency (normalized to the maximum plasma frequency) at 2, 6, and 15 GHz for the lineout shown in Figure 4.

The sampled collision frequencies correspond to neutral densities of (0, 10^{23},10^{24}, 5×10^{24}, 10^{25}) m^{-3}. Because the plasma profile is thicker than the simple geometry discussed in Section IV, we find that larger values of the neutral density are needed to obtain a signal that could possibly be measured. In Figure 5, the star symbols for the 2 GHz and 6 GHz RF sources indicate that no measured signal transmits through the sheath. In Figure 5, we observe a similar trend with a realistic sheath profile that we observe in Figure 3. Specifically, as neutral density increases, transmission increases at all RF frequencies. Furthermore, we observe that the improvement in transmission increases as RF frequency decreases, which is consistent with the theory and simulation results of the ideal profile shown in Figure 3.

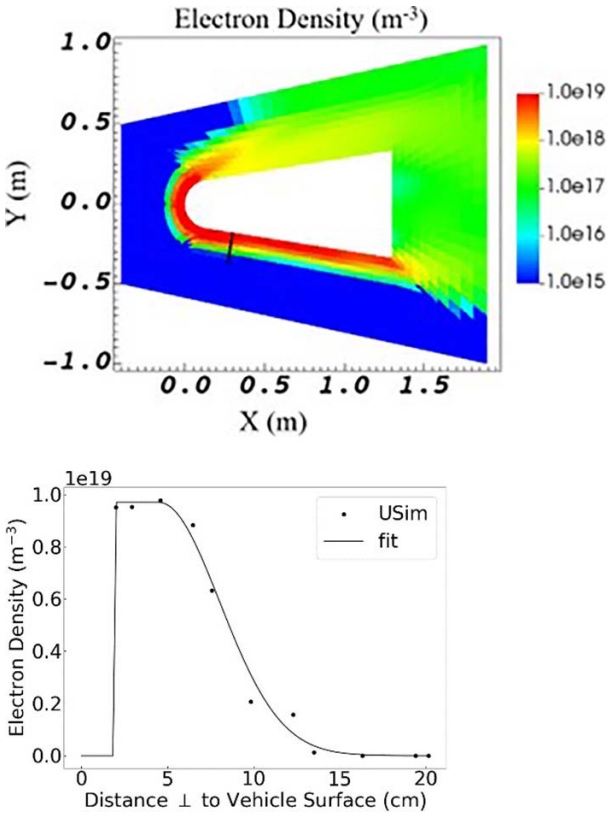

Figure 4. (top) Two-dimensional cross section of the electron density from a three-dimensional computational fluid dynamics simulation [13]. (bottom) Lineout of the density in the top panel.

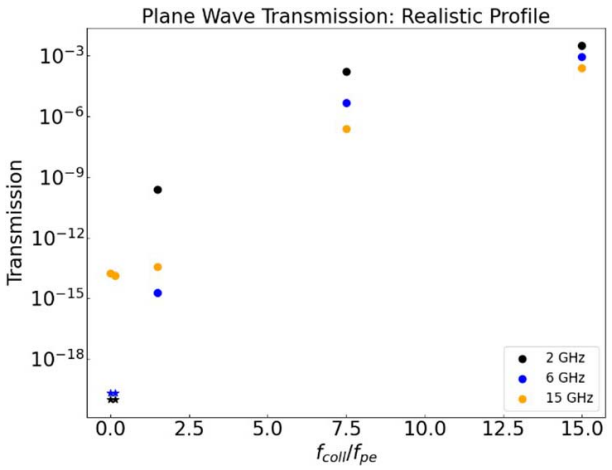

Figure 5. RF transmission through the black profile shown in Figure. 4. The horizontal scale is normalized to the maximum plasma frequency. The blue and black stars indicate that the noise was too great to measure a discernable signal at 2 GHz and 6 GHz.

6. Conclusion

We have shown that the effect of electron-neutral collisions in a dense plasma is to improve transmission for source frequencies less than the plasma frequency. We further show that the improvement is greater at lower frequencies, which is a result consistent with theory if the plasma is modeled as a conducting material for frequencies below the plasma frequency. Our work is consistent with [13], where it was found that attenuation through a plasma is proportional to $\sqrt{f_p}/v$ for a magnetic field source and for scenarios of $200 < \frac{f_p}{f} < 30,000$. Here we show this relationship for the general case and for scenarios where plasma frequency is only a few factors greater than radio frequency, which is more relevant to L-band and S-band signals.

A consequence of the results herein is that for fixed plasma frequency and communication frequency necessarily less than the plasma frequency, it is advantageous to maximize collisions and decrease communication frequency in order to improve transmission through the plasma. The collision frequency can be increased by lowering altitude, intentionally injecting additional neutral molecules, or leveraging temperature dependence of the collision frequency in plasmas. This approach is dubbed the "collision frequency window" and is an additional tool to mitigate plasma-induced radio blackout and other scenarios.

7. References

1. R. A. Hartunian, G. E. Stewart, S. D. Fergason, T. J. Curtiss, and R. W. Seibold, "Causes and Mitigation of Radio Frequency (RF) Blackout During Reentry of Reusable Launch Vehicles," Report DOT-VNTSC-FAA-06-23, Aerospace Corp, El Segundo, CA, USA, January 2007.
2. P. Garg and A. K. Dodiyal, "Reducing RF Blackout During Re-Entry of the Reusable Launch Vehicle," 2009 IEEE Aerospace Conference, Big Sky, MT, USA, March 7, 2009.
3. E. D. Gillman, J. E. Foster, and I. M. Blankson, "Review of Leading Approaches for Mitigating Hypersonic Vehicle Communications Blackout and a Method of Ceramic Particulate Injection via Cathode Spot Arcs for Blackout Mitigation," No. NASA/TM-2010-216220, 2010.
4. C. Thoma, D. V. Rose, C. L. Miller, R. E. Clark, and T. P. Hughes, "Electromagnetic Wave Propagation Through an Overdense Magnetized Collisional Plasma Layer," *Journal of Applied Physics*, **106**, 4, August 2009, p. 043301.
5. H. L. Caldelas II, *Experimental Design of Electrophilic Gas Injection System for Plasma Blackout Mitigation During Hypersonic Reentry*, Ph.D. dissertation, Massachusetts Institute Technology, Cambridge, MA, USA, 2021.
6. B. A. Webb and R. W. Ziolkowski, "A Metamaterial-Inspired Approach to Mitigating Radio Frequency Blackout When a Plasma Forms Around a Reentry Vehicle," *Photonics*, **7**, 4, October 2020, p. 88.
7. S. Schelkunoff, "The Impedance Concept and Its Application to Problems of Reflection, Refraction, Shielding, and Power Absorption," *Bell System Technical Journal*, **17**, 1, January 1938, pp. 17-48.
8. C. Nieter and J. R. Carry, "Vorpal: A Versatile Plasma Simulation Code," *Journal of Computational Physics*, **196**, 2, May 2004, pp. 448-473.
9. D. N. Smithe, "Finite-Difference Time-Domain Simulation of Fusion Plasmas at Radio Frequency Time Scales," *Physics of Plasma*, **14**, 5, May 2007, p. 056104.
10. A. F. Oskooi, L. Zhang, Y. Avniel, and S. G Johnson, "The Failure of Perfectly Matched Layers, and Towards Their Redemption by Adiabatic Absorbers," *Optics Express*, **16**, 15, July 2008, pp. 11376-11392.
11. M. Kundrapu, J. Loverich, K. Beckwith, P. Stoltz, A. Shashurin, et al., "Modeling Radio Communication Blackout and Blackout Mitigation in Hypersonic Vehicles," *Journal of Spacecraft and Rockets*, **52**, 3, 2015 pp. 853-862.
12. J. Loverich, S. D. Zhou, K. Beckwith, M. Kundrapu, M. Loh, et al. "Nautilus: A Tool for Modeling Fluid Plasmas," AIAA Paper 2013-1185, 51st AIAA Aerospace Sciences Meeting Including the New Horizons Forum and Aerospace Exposition, Grapevine, TX, USA, January 5, 2013.
13. D. L. Liu, X. P. Li, Y. M. Liu, K. Xie, and B. W. Bai, "Attenuation of Low-Frequency Electromagnetic Wave in the Thin Sheath Enveloping a High-Speed Vehicle upon Re-Entry," *Journal of Applied Physics*, **121**, 7, 2017, p. 074903.